Author Manuscript

Author Manuscript

Author Manuscript

Author Manuscript

HHS Public Access

Author manuscript

IEEE Trans Med Robot Bionics. Author manuscript; available in PMC 2022 August 01.

Published in final edited form as:

IEEE Trans Med Robot Bionics. 2021 August ; 3(3): 563–572. doi:10.1109/TMRB.2021.3098952.

Acquisition of Surface EMG Using Flexible and Low-Profile Electrodes for Lower Extremity Neuroprosthetic Control

Seong Ho Yeon[1], **Tony Shu**[1], **Hyungeun Song**[3], **Tsung-Han Hsieh**[1], **Junqing Qiao**[1], **Emily A. Rogers**[2], **Samantha Gutierrez-Arango**[1], **Erica Israel**[1], **Lisa E. Freed**[1], **Hugh M. Herr**[1]

[1]MIT Program in Media Arts and Sciences, and the MIT Center for Extreme Bionics, Massachusetts Institute of Technology, Cambridge, MA 02139 USA.

[2]MIT Department of Mechanical Engineering, and the MIT Center for Extreme Bionics, Massachusetts Institute of Technology, Cambridge, MA 02139 USA.

[3]MIT Health Sciences and Technology Program, and the MIT Center for Extreme Bionics, Massachusetts Institute of Technology, Cambridge, MA 02139 USA.

Abstract

For persons with lower extremity (LE) amputation, acquisition of surface electromyography (sEMG) from within the prosthetic socket remains a significant challenge due to the dynamic loads experienced during the gait cycle. However, these signals are critical for both understanding the clinical effects of LE amputation and determining the desired control trajectories of active LE prostheses. Current solutions for collecting within-socket sEMG are generally (i) incompatible with a subject's prescribed prosthetic socket and liners, (ii) uncomfortable, and (iii) expensive. This study presents an alternative within-socket sEMG acquisition paradigm using a novel flexible and low-profile electrode. First, the practical performance of this Sub-Liner Interface for Prosthetics (SLIP) electrode is compared to that of commercial Ag/AgCl electrodes within a cohort of subjects without amputation. Then, the corresponding SLIP electrode sEMG acquisition paradigm is implemented in a single subject with unilateral transtibial amputation performing unconstrained movements and walking on level ground. Finally, a quantitative questionnaire characterizes subjective comfort for SLIP electrode and commercial Ag/AgCl electrode instrumentation setups. Quantitative analyses suggest comparable signal qualities between SLIP and Ag/AgCl electrodes while qualitative analyses suggest the feasibility of using the SLIP electrode for real-time sEMG data collection from load-bearing, ambulatory subjects with LE amputation.

Corresponding author: Hugh Herr hherr@media.mit.edu, MIT Program in Media Arts and Sciences, and the MIT Center for Extreme Bionics, Massachusetts Institute of Technology, Cambridge, MA 02139 USA.

AUTHOR CONTRIBUTIONS

S.H.Y. and H.M.H. conceived of the study. S.H.Y. developed and fabricated the SLIP electrode and embedded sEMG acquisition system. S.H.Y., T.S., T.H., and E.A.R. contributed to system integration of the sEMG acquisition equipment. T.S. conceived and planned the experiment for quantitative evaluation of the SLIP electrode. S.H.Y. and T.S. performed quantitative evaluation of the SLIP electrode. All authors planned and performed the qualitative evaluations of the SLIP electrode. S.H.Y., T.S., H.S., T.H., E.A.R., L.E.F., and H.M.H. contributed to writing the manuscript. H.M.H. supervised the project.

Author Manuscript Author Manuscript Author Manuscript Author Manuscript

I. INTRODUCTION

Surface electromyography (sEMG), the least invasive technique among current peripheral neural interface technologies, is one of the most deeply researched and clinically viable methods for extrinsic neural control of prosthetic devices [1]–[4]. With the advancement of novel surgical amputation paradigms such as Targeted Muscle Reinnervation (TMR) and the Agonist-Antagonist Myoneural interface (AMI), the efficacy and utility of sEMG-based control approaches has drastically increased in applications related to advanced neuroprosthetic systems [5], [6].

However, while sEMG has been widely applied to control upper extremity neuroprostheses, relatively fewer studies have explored sEMG control of lower extremity (LE) neuroprostheses, a disparity that Windrich et al. attribute to unique implementation challenges within the application domain [7]. This study specifically addresses sEMG acquisition within the LE prosthetic liner, a task whose difficulties are most pronounced during ambulatory activity when a residual limb experiences extreme dynamic pressure changes that cause structural deformation, electrode contact variation, pain, and additive sEMG signal noise. A solution for within-socket sEMG acquisition may inform subsequent solutions for downstream challenges, including the need for a high-powered portable actuator design, a suitable neural control paradigm for ambulatory activity, and an optimal prosthetic socket design [8].

Several previous studies have successfully used sEMG signals from the residual limb to determine unconstrained neuroprosthetic movements in free space [9]–[12]. To further explore sEMG as a control signal during ambulation, others have attempted to place commercial pre-amplifiers inside the prosthetic liner within the socket [6], [13], [14]. While this approach has been shown to successfully acquire sEMG data, the bulkiness of the pre-amplifiers creates painful indentations on the skin which make it unsuitable for long-term use and translation beyond clinical trials. Another alternative paradigm involves modifying existing or prototyping experimental prosthetic sockets and liners with embedded, minimally-protruding electrodes [15]–[20]. However, the necessity of fabricating a customized socket and liner for each individual subject is often both too time-consuming and prohibitively expensive for practical purposes.

In consideration of these engineering trade-offs, we propose an efficient and cost-effective method for sEMG acquisition within lower extremity prosthetic sockets using a novel, flexible, and low-profile electrode design. Importantly, the design is intended to be compatible with a user's existing socket and liner without modification. In this study, we demonstrate the capability of these custom Sub-Liner Interface for Prosthetics (SLIP) electrodes to provide useful sEMG signals from the residual limb under dynamic load-bearing conditions. The flexible and thin nature of the custom electrodes minimizes skin indentation within the socket, especially compared to the methods with pre-amplifier dependencies from previous literature. Furthermore, SLIP electrodes can be readily fabricated with flexible printed-circuit-board (fPCB) technology at low cost. As a research tool, the SLIP electrode design may faciliate accelerated development of neuroprosthetic systems as a whole, and while not yet clinical grade, it introduces a general paradigm

Author Manuscript Author Manuscript Author Manuscript Author Manuscript

of sEMG collection which may have potential applications in translational neuroprosthetic systems due to the engineering advantages discussed.

The paper is organized as follows: Section II introduces the design of the novel electrode, including sEMG acquisition setup and processing. Section III quantitatively evaluates the SLIP electrode by evaluating signal interchangeability with those recorded from commercial Ag/AgCl electrodes in subjects without amputation. Section IV demonstrates an application of the custom electrodes in a subject with unilateral transtibial amputation while seated and while ambulating. Section V evaluates relative comfort between SLIP and Ag/AgCl electrodes. Finally, Section VI provides discussion and conclusions. This work is extended from a previous study by Yeon et al. [21].

II. METHODS:

Design of the Flexible and Low-Profile Electrode

A. Design Criteria—The SLIP electrode is designed to overcome current challenges regarding utilization of sEMG-based control of LE neuroprostheses in clinical trials. Specifically, the SLIP electrode design addresses three technical challenges:

- *Compatibility with standard sockets and liners*: As discussed in Section I, sEMG acquisition using custom subject-specific liners and sockets incurs high costs and requires significant lead times. Developing an electrode technology compatible with traditional sockets and liners would enable researchers to conduct experiments more efficiently from both of these perspectives.
- *Subject comfort*: Prior research applications using commercial electrode technology to measure sEMG signals inside load-bearing sockets were primarily limited by subjects' discomfort and pain. Subject comfort is critical in both research and translational applications [6], [13], [14].
- *Manufacturability*: Using standard fPCB electronics fabrication technologies to produce the SLIP electrode itself minimizes cost and lead time when ordering in bulk from readily-available vendors.

These design requirements for compatibility, comfort, and manufacturability are necessary for increasing research productivity and decreasing the cost of human subject experiments.

B. Related Technologies—Several research attempts have been made to develop flexible and dry surface electrodes for electroencephalogram (EEG), electrocardiogram (ECG) and EMG acquisition [22]–[30]. This push for flexible and dry electrode technology is driven by the desire for long-term biopotential monitoring that extends beyond the lifespan of typical wet Ag/AgCl electrodes [22]–[27]. By using various substrate materials such as polydimethysiloaxane (PDMS) and parylene, these efforts successfully demonstrated that flexible and dry electrodes can obtain signal qualities comparable to Ag/AgCl electrodes. A couple of these attempts were also able to develop electrodes with minimal thickness ($< 300 um$) [27], [28].

Author Manuscript Author Manuscript Author Manuscript Author Manuscript

Nonetheless, most of these technologies remain too fragile or difficult to manufacture and are not directly translatable to LE prosthesis applications.

C. Design Concept—A conceptual diagram of the SLIP electrode design, including form factor and usage, is shown in Fig. 1 with additional design details being provided in the following subsections.

The SLIP electrode was designed for insertion between a subject's residuum and prosthetic liner. As thinner profiles were hypothesized to provide better user comfort and experience, electrode profile height was minimized. Given limitations in manufacturing capabilities, the profile height of the prototype electrode is slightly less than 100 μm. An insulated trace originating from the electrode contact heads leads to a terminal electrical connector that interfaces with a portable sEMG amplifier and processor mounted externally on the socket. This feature allows subjects to use their own prosthetic socket and liner without modifications.

D. Electrical and Mechanical Design—The shape of the electrode head was designed based on bipolar sEMG electrode guidelines from the European project Surface EMG for Non-Invasive Assessment of Muscles (SENIAM) [31]. The electrical CAD model of the electrode skin contact is shown in Fig. 2. Each bipolar electrode is circular with a diameter of 10 mm [31], [32]. An inter-electrode distance of 16 mm was chosen after considering the effects of inter-muscle crosstalk and differential sEMG signal power [33]. The electrical connections inside the electrode were routed according to differential signal routing standards for maximizing common mode rejection. Only a single layer of copper metal was utilized in order to minimize thickness and maximize flexibility of the electrode. Thread holes were placed on the electrode head and around the lead wire for potential mechanical integration with a prosthetic liner or sock by sewing. This approach would provide a semi-permanent installation for ease of donning and doffing the electrodes during repeated trials.

Table I summarizes the design specifications of the SLIP electrode. Notably, the connector type and length of the electrode can be varied based on application. These design decisions are not necessarily optimal, but do represent efficient and convenient selections.

E. Materials and Manufacturability—Materials were chosen for compatibility with standard flexible PCB manufacturing techniques to increase accessibility for researchers. Details of the selected materials are shown in Table II.

Polyimide (PI) film was used as a base substrate. PI film is one of the most commonly used insulating substrates in fPCB fabrication. Material safety data sheets for PI report that "no skin irritation is expected from handling film [34]."

The copper layer is gold-plated where exposed to improve sensor compatibility with the skin. While a thorough compatibility evaluation of the novel electrode with skin is beyond the scope of this paper, a growing body of literature suggests electrodes with PI substrates

Author Manuscript Author Manuscript Author Manuscript Author Manuscript

and gold contacts, including electrode implants, are compatible with long-term usage [35], [36].

F. Manufactured Prototype—The prototype SLIP electrode was fabricated by an international fPCB vendor (PCBWay, Xiacheng District, Hangzhou, China) using generic fPCB fabrication techniques. The fabricated electrode is shown in Fig. 3. The manufactured flexible electrode costs less than $6.00 per sensor when purchased in quantities of 30. The per-electrode cost can be greatly reduced if purchased in larger quantities.

III. EXPERIMENT A:

Quantitative Evaluation of the SLIP Electrode

A. Subject Recruitment and Study Preparation—To evaluate the measurement characteristics of the SLIP electrode, five subjects (18–22 years old; three male, two female) with no amputation and no self-reported neuromuscular pathologies were recruited. Subjects provided written informed consent through MIT Committee on the Use of Humans as Experimental Subjects (COUHES) protocol #1906898371.

In a cross-validation study, a pair of commercially-available Ag/AgCl electrodes was placed alongside the SLIP electrode to measure bipolar sEMG from the left leg's tibialis anterior (TA) during free space movements, as seen in Fig. 4. Ag/AgCl electrode chemistry was selected for comparison against the SLIP electrode due to its standardized use in sEMG acquisition [31]. The SLIP electrode was fixed to the skin with adhesive tape before applying uniform pressure to all electrodes using an elastic exercise band, as seen in Fig. 4b. The location of the muscle belly was estimated through palpation, and Ag/AgCl inter-electrode spacing was matched to the fixed spacing of the SLIP electrode. Because sEMG measurements are sensitive to the locations of electrodes relative to underlying muscle, the commercial wet electrodes' and the SLIP electrode's relative positioning on the limb was alternated between medial and lateral positions over the estimated location of the TA belly from subject to subject, as inspired by a study comparing two types of wet surface electrodes by Posada-Quintero et al. [37]. The TA was selected for analysis due to its proximity to the skin surface and corresponding ease of access. The low amount of subcutaneous fat superficial to the TA minimized the attenuation of sEMG signals for all subjects.

B. sEMG Instrumentation—Specification of the sEMG acquisition hardware is informed by qualitative assessment of generic electrical characteristics pertinent to the SLIP electrode. The SLIP electrode has a dry metal contact surface that results in higher skin-electrode impedance compared to that of Ag/AgCl electrodes [22]. Because of the dry interface between SLIP electrode and skin, the impedance of the system can vary with dynamic differential pressure changes that result in DC voltage swings an order-of-magnitude higher than the amplitude of the EMG signal. Moreover, due to the proposed acquisition architecture, raw sEMG signals need to be transferred over a relatively long-distance ($> 40\ cm$) before interfacing with the analog-front-end (AFE) IC. Due to the single metal layer within the electrode, various methods to protect the sEMG signal through electrical shielding were not available for our applications [38].

Author Manuscript Author Manuscript Author Manuscript Author Manuscript

Therefore, the AFE with a DC-coupled differential pre-amplifier (AD8422., Analog Devices, Norwood, MA, USA) with high input impedance ($Z_{in} = 200G\Omega\text{k} \parallel 2pF$) and low gain ($G = 10$) was utilized in order to mitigate the high skin-electrode impedance and large dynamic DC voltage swings anticipated. Along with the pre-amplifier, a 24-bit high resolution analog-to-digital-converter (ADC) IC (ADS1299., Texas Instrument, Dallas, TX, USA) was utilized for sEMG signal acquisition. Fig. 5 shows the custom embedded sEMG acquisition platform used in this experiment session [39].

C. Data Collection—While seated and starting from a neutral ankle position, subjects performed five trials each of ankle dorsiflexion and ankle cocontraction in free space to generate raw bipolar sEMG data. Ankle dorsiflexion trials required subjects to fully dorsiflex their left ankle and hold the position. Ankle cocontraction trials required subjects to hold their left ankle in a neutral position while cocontracting associated muscles to increase the stiffness of the joint. In chronological order, each guided trial consisted of three seconds of rest, three seconds of activity, and three seconds of rest. Within these trials, raw sEMG signals were sampled and logged at a frequency of 1 kHZ.

D. Data Analysis—Data collected from commercial Ag/AgCl electrodes and the SLIP electrode were analyzed in the time domain to determine their interchangeability for the purposes of neuro-prosthesis control. Namely, we measured muscle activation onset/offset times and Pearson's correlation of discrete muscle activation envelopes between electrode types in a manner similar to Posada-Quintero et al. [37]. The practical control implication of identical onset/offset times and a unity Pearson's correlation would be a neuroprosthesis that is identically controlled using either type of electrode.

To obtain a linear envelope of sEMG roughly corresponding to muscle activation, all signals were first forward-backward filtered using a 4th-order Butterworth filter designed in MATLAB *ver. R2019b* (MathWorks, Inc., Natick, MA, USA) with a passband of 80 – 400 Hz. Passband thresholds were chosen to remove 60 Hz mains hum, motion artifacts, and high frequency noise [40]. Signals were then rectified and subjected to a moving average filter with a window length of 150 ms. Normalization was performed within each trial on each channel's resulting waveform by dividing all voltages by the maximum voltage recorded on that channel. Applying a moving average filter to processed sEMG for an online estimate of muscle activation in this manner is widely used within the domain of neuromuscular modeling.

- *Muscle on- and off-times*: The linear envelope of sEMG was used to estimate on- and off-times for muscle contraction during each trial. A single threshold was used to determine both time indices, specified by

$$Threshold = \mu + 6\sigma \tag{1}$$

where μ and σ are the mean and standard deviation of the linear envelope during the first second of rest at the beginning of each trial. Due to the orders of magnitude difference between quiescent noise and true muscle activation, a 6σ threshold was chosen to conservatively define an absolute noise floor and avoid false detection of onset muscle activation. Onset and offset timings of the linear

Author Manuscript Author Manuscript Author Manuscript Author Manuscript

envelope measured by the SLIP electrode relative to the Ag/AgCl electrodes were compared in a Bland-Altman plot. Individual trials were systematically excluded from analysis if the linear sEMG envelope exceeded four seconds. These trials typically contained low amplitude sEMG peaks after the main sEMG envelope that made offset time indeterminate, indicative of the subject's failure to fully relax according to instructions.

- *Pearson's correlations*: For each trial, Pearson's correlations were calculated between the linear envelopes of sEMG measured by the SLIP electrode and Ag/AgCl electrodes between average on-time and average off-time.

E. Quantitative Results—Relative muscle on- and off-times suggest a high degree of agreement between the SLIP electrode and commercial Ag/AgCl electrodes, as seen visually in Fig. 6. Representative linear envelopes of muscle activity (a) measured by both commercially available Ag/AgCl electrodes and the SLIP electrode are shown in Fig. 7. Envelope correlations between Ag/AgCl and flexible electrodes also suggest high degree of agreement. The group average Pearson's correlation coefficient for qualified dorsiflexion trials ($n = 22$) was 0.95 ± 0.92 (average ± std. dev.). The group average Pearson's correlation coefficient for qualified cocontraction trials ($n = 21$) was 0.94 ± 0.04.

IV. EXPERIMENT B:

sEMG Acquisition within Lower Extremity Prosthetic Systems

A. Subject Recruitment—To evaluate the efficacy of the novel electrodes within a load-bearing prosthetic socket, a single subject (43 years old, female) with unilateral left-side transtibial amputation was recruited. The subject's amputation was performed under the novel Agonist-antagonist Myoneural Interface (AMI) surgical paradigm, forming two dynamically coupled agonist-antagonist muscle pairs—tibialis anterior (TA) paired with lateral gastrocnemius (LG), and tibialis posterior (TP) paired with peroneous longus (PL)—within the residuum [6]. The subject provided written informed consent through MIT COUHES protocol #1812634918.

B. Physical Placement of the Electrode—Proper physical placement of the electrode is required for user comfort as well as high signal quality. Specifically, because the SLIP electrode interfaces with the pre-amplifer outside of the socket after a relatively long transmission distance, it is important to isolate the signal from additional parasitic electrical elements. Because AMI muscles are readily palpable and precisely locatable, only four SLIP electrodes were required for this specific experimental section. However, for demonstrative purposes, Fig. 8 presents a generic skin preparation and fully-instrumented electrode placement process.

Elastic Kinesio tape and hydrocolloidal matrix bandages were used to ensure good mechanical anchoring of the electrode on the skin within the liner environment. The compliance of the bandages is hypothesized to support continuous contact between electrodes and skin surface during dynamic pressure changes so as to minimize skin-electrode impedance.

Author Manuscript Author Manuscript Author Manuscript Author Manuscript

Additionally, the wires of the electrodes were necessarily routed along the longitudinal plane of the residual limb toward the proximal end of the liner. In areas where the residual limb and liner experience bending, such as the knee joint, it is crucial to minimize friction between leads and skin. To mitigate this issue, a prosthetic sock was placed between the electrode wires and skin with electrode leads passing through small incisions in the sock.

C. sEMG Instrumentation and Data Processing—A custom embedded sEMG acquisition system was utilized to measure signals from within the LE prosthetic liner in this experiment session. The specific embedded sEMG system is an improved version of the sEMG system from Section III: Experiment A that enables simultaneous measurement of 16 channels at an increased sampling rate of 2 kHz [39]. The sEMG system retains an identical AFE structure compared to the previous version. For demonstrative purposes, Fig. 9 presents a fully-instrumented example use case wherein electrode leads exiting the prosthetic liner are interfaced with the sEMG system through the FFC connector adapter.

The sampled sEMG signals were band-pass filtered with a pass-band of 80 ~ 340 Hz, rectified with a root-mean-square (RMS) operation, and summed within a 200 ms time window. When processing sEMG signals collected during ambulation, additional cumulative histogram filtering (CHF) process was performed to mitigate artifacts from dynamic ground impacts [41]. A cumulative short-time histogram within a summation time window was first calculated, and a subsequent RMS operation was applied to the data points that fell within the 10% to 80% range of signals in the cumulative histogram.

D. Experiment Design and Data Collection—For this experiment specifically, four SLIP sEMG electrodes were applied to the residual limb to instrument the targeted AMI muscle pairs without channel redundancy.

In the first session, the subject was asked to rotate her phantom limb in a clockwise direction while seated and actively contracting each AMI muscle pair. Then, the subject was asked to walk on an instrumented, split-belt treadmill (Bertec Corporation, Columbus OH) using a passive prosthetic ankle at a speed of 1.4 m/s. Two independent force plates under the split-belt treadmill recorded ground reaction force (GRF) data at a sampling rate of 1 kHz. The GRF data for the affected left side were subsequently processed with a 10 ms window median filter. The GRF for the intact right side are not reported here. Raw sEMG data were wirelessly logged during the experiment via a WIFI module (RN42., Microchip Technology, Chandler, AZ) at a frequency of 2kHz. Fig. 10 shows the sEMG acquisition setup for ambulation with the SLIP electrodes connected to the liner-mounted sEMG system.

E. Qualitative Results

1. *Stationary Voluntary Movement:* The normalized sEMG signals measured from the residual limb during voluntary rotation of the phantom ankle and subtalar joints are shown in Fig. 11. A distinct sEMG activation pattern was clearly observed with high signal-to-noise ratio, as can be seen in the contrast between periods of rest and periods of activity. For each cycle of rotation, reciprocal activation patterns for each AMI muscle pair were observed which correlated with rotation of the phantom limb. The distinct patterns and high signal quality

Author Manuscript Author Manuscript Author Manuscript Author Manuscript

observed can be reasonably considered sufficient for various applications of sEMG, including closed-loop control of neuroprosthetic devices.

2. *Ambulation:* The normalized sEMG signals from the residual limb of the subject during ambulation are shown in Fig. 12. Measured ground reaction forces correlated with sEMG signals showed clear swing and stance phases within the gait cycle. During the gait cycle, repetitive muscle activation patterns for each muscle were clearly observed in the recorded data. Notably, sEMG activation patterns of an amputated residual limb are not identical to those of an intact limb, and the subject was additionally amputated with the novel AMI amputation paradigm [6], [15]. In these results, the ground truth of the desired muscle activation patterns from AMI musculature is unknown, and direct comparison and evaluation of the sEMG signals based upon physiological musculature is challenging. However, cyclic and repetitive activation patterns synchronized with gait cycle ground reaction forces suggest the potential for their use in neuroprosthetic control.

F. Post-Ambulation Skin Evaluation—As stated in Section II, subject comfort was one of the critical criteria when designing the SLIP electrode. Fig. 13 shows the appearance of the residuum after doffing the prosthetic socket and liner following over an hour of load-bearing activities. Purple marker outlines on the skin indicate the locations of the placed electrodes. Given the well-documented challenges to comfortably access muscles inside load-bearing sockets, this preliminary finding demonstrates minimal, if any, observable skin indentation due to the novel electrodes.

V. EXPERIMENT C:

User Comfort Evaluation

A. Subject Recruitment and Experiment Design—To determine the practical feasibility of collecting sEMG data using the commercial Ag/AgCl electrodes within a load-bearing prosthetic socket, the same subject (43 years old, female) with unilateral transtibial AMI amputation was recruited for a third experimental section. This set of experiments was designed to provide a quantified comparison of relative comfort. The subject provided written informed consent through MIT COUHES protocol #1812634918.

For each of the subsequent three experiments, four bipolar pairs of electrodes in various configurations were acutely placed superior the muscle bellies of the TA, LG, TP, and PL muscles. Three electrode configurations were investigated, involving: 1) the SLIP electrode, 2) the Ag/AgCl disposable electrode alone, and 3) the Ag/AgCl electrode with requisite connector and wires, respectively, as shown in Fig. 14. Configuration 2 represents an ideal use case involving commercial wet electrodes in which customized wire leads are fully embedded into the socket liner. Configuration 3 represents a typical use case involving commercial wet electrodes with commercial wire leads that are connected to an external sEMG recording system.

Author Manuscript Author Manuscript Author Manuscript Author Manuscript

For each electrode configuration, a progressive series of tasks was presented to the user to test comfort in typical real-world scenarios. First, the patient was asked to don her prosthesis with the electrodes attached to the limb and remain seated for 15 mins. After 15 mins, the subject was asked to perform multiple motor tasks, including sitting, standing, walking (1.4 m/s), stair ascent, and stair descent. Finally, the subject was asked to report her subjective comfort and level of socket suspension, and preference for daily life usage on a 1–5 scale. If the subject indicated any significant discomfort at any point, the specific trial was stopped immediately and a '1 = not applicable' score was given for that section.

B. Reported Comfort and Preference Scores—The comfort and preference scores reported by the subject are given in Table III. The reported scores showed that the SLIP electrodes caused no noticeable differences in comfort compared to wearing the prescribed prosthesis without electrodes over a wide range of movements. The subject reported that even detecting the presence of the electrodes was "extremely challenging", and she would be fully willing to use SLIP electrodes if they were able to provide volitional control of her prosthesis. Notably, Configuration 2, which involved only Ag/AgCl electrodes, elicited only a slight increase in discomfort. However, the subject reported the ability to feel each of the conventional Ag/AgCl electrodes within socket. Furthermore, the subject noted that these Ag/AgCl electrodes were applying pressure to the point of affecting circulation within the residual limb. During testing of Configuration 3, the subject reported severe discomfort during initial sock donning and was not able to proceed with any of given tasks.

VI. DISCUSSION

This study investigated an effective and economical method of acquiring sEMG signals from the weight-bearing LE residual limb within the donned prosthetic liner and socket. The unique challenges presented by dynamic loading inside the prosthetic socket during gait have limited the applications of traditional sEMG acquisition techniques in the LE domain. Here, some of these challenges were addressed using flexible, low-profile SLIP electrodes. In a quantitative comparison of five subjects without amputation or LE pathology, SLIP electrodes produced muscle activation signals which were interchangeable with those recorded with commercial Ag/AgCl electrodes. When tested in a subject with an LE amputation during walking, the SLIP electrodes were found to be compatible with her prosthetic socket and liner, and did not cause any discomfort or skin indentation.

With the caveat that the present walking study included only one single subject who had received an AMI transtibial amputation, it was remarkable to observe periodic activity of antagonistic residual limb muscle pairs (TA-LG and PL-TP) that appeared to be entrained to the gait cycle. In contrast, a previous study reported muscle activation patterns that were aperiodic despite subject entrainment into a gait cycle in subjects who had undergone standard transtibial amputations [13]. Additionally, due to their flexible and low-profile nature, the SLIP electrodes were shown to be compatible with the subject's prescribed lower extremity prosthetic socket and liner without any discomfort and skin indentation. These characteristic of the SLIP electrodes allowed for confident measurement of signals which are potentially appropriate for neuroprosthetic control. However, additional extensive studies are

Author Manuscript Author Manuscript Author Manuscript Author Manuscript

still required to quantify their sensitivity to impact artifacts and understand the physiological basis for the observed sEMG patterns.

While the proposed SLIP electrode sEMG acquisition paradigm tentatively demonstrates utility in LE prosthetic applications, future work should expand to consider the compatibility of the paradigm in other,varied domains and application contexts. Due to the unique requirements of LE prosthetic systems, the SLIP electrode's engineering concessions include its dry nature, potential susceptibility to mechanical perturbation, and lack of electrical shielding. Thus, as mentioned in Section II, the SLIP electrodes require proper pairing with a high-end sEMG processor AFE.

Although only four channels were presented for analysis during the gait portion of this study, the potential exists for extracting additional information from all sixteen channels. In particular, because measured signals are sensitive to environmental variables such as electrode placement and sweat, among other factors, machining learning techniques that do not require explicit labeling of muscles or other underlying assumptions may prove effective when applying the collected signals toward volitional control of a powered prosthesis during gait. The high level of channel redundancy provided by the flexible electrode system proposed in this manuscript, previously unavailable for practical reasons, presents the prosthesis researcher with new directions of investigation. For example, future investigations may analyze the performance of combinations of multiple signal processing techniques and controller models in movement-based tasks.

Based upon the preliminary quantitative and qualitative evaluations, the novel electrodes described in this study appear capable of robust sEMG signal acquisition from within a LE prosthetic socket and liner, adding to a growing body of literature focused on EMG-based control neuroprosthetic control that is more typically demonstrated in subjects living with upper limb upper extremity amputations [42]–[45]. The main limitation of this study is the small number of test subjects; this limitation is being addressed in ongoing studies. Also, although the novel SLIP electrode was designed with safety considerations in mind, it is important to emphasize that usage has been limited to relatively short test sessions, and long-term compatibility studies are warranted. Nonetheless, the authors hope that the proposed sEMG acquisition method will facilitate the process of human subject trials in the field of LE neuroprostheses, including the application of measured sEMG signals toward control of active prostheses in real-world tasks.

ACKNOWLEDGMENT

The authors thank J.F. Duval for his advice and support on electronics design. The authors also thank the reviewers for their invaluable comments which have improved the paper substantially.

This work was supported by the MIT Media Lab Consortia and *Eunice Kennedy Shriver National Institute of Child Health & Human Development of the National Institutes of Health (NIH)* under award number R01HD097135. The content is solely the responsibility of the authors and does not necessarily represent the official views of the NIH.

Author Manuscript Author Manuscript Author Manuscript Author Manuscript

References

[1]. Tucker MR, Olivier J, Pagel A, Bleuler H, Bouri M, Lambercy O, Millán J, Riener R, Vallery H, and Gassert R., "Control strategies for active lower extremity prosthetics and orthotics: a review," Journal of neuroengineering and rehabilitation, vol. 12, no. 1, p. 1, 2015. [PubMed: 25557982]

[2]. De Luca CJ, "The use of surface electromyography in biomechanics," Journal of applied biomechanics, vol. 13, no. 2, pp. 135–163, 1997.

[3]. Farina D, Merletti R, and Enoka RM, "The extraction of neural strategies from the surface emg: an update," Journal of Applied Physiology, vol. 117, no. 11, pp. 1215–1230, 2014. [PubMed: 25277737]

[4]. Jiang N, Dosen S, Muller K-R, and Farina D., "Myoelectric control of artificial limbsâĂŤis there a need to change focus?[in the spotlight]," IEEE Signal Processing Magazine, vol. 29, no. 5, pp. 152–150, 2012.

[5]. Kuiken TA, Li G, Lock BA, Lipschutz RD, Miller LA, Stubblefield KA, and Englehart K., "Targeted muscle reinnervation for real-time myoelectric control of multifunction artificial arms," The Journal of the American Medical Association, vol. 301, no. 6, pp. 619–628, 2009. [PubMed: 19211469]

[6]. Clites TR, Carty MJ, Ullauri JB, Carney ME, Mooney LM, Duval J-F, Srinivasan SS, and Herr HM, "Proprioception from a neurally controlled lower-extremity prosthesis," Science Translational Medicine, vol. 10, no. 443, 2018.

[7]. Windrich M, Grimmer M, Christ O, Rinderknecht S, and Beckerle P., "Active lower limb prosthetics: a systematic review of design issues and solutions," Biomedical engineering online, vol. 15, no. 3, p. 140, 2016. [PubMed: 28105948]

[8]. Paternò L, Ibrahimi M, Gruppioni E, Menciassi A, and Ricotti L., "Sockets for limb prostheses: a review of existing technologies and open challenges," IEEE Transactions on Biomedical Engineering, vol. 65, no. 9, pp. 1996–2010, 2018. [PubMed: 29993506]

[9]. Hargrove LJ, Simon AM, Lipschutz R, Finucane SB, and Kuiken TA, "Non-weight-bearing neural control of a powered transfemoral prosthesis," Journal of neuroengineering and rehabilitation, vol. 10, no. 1, pp. 1–11, 2013. [PubMed: 23336711]

[10]. Au SK, Bonato P, and Herr H, "An emg-position controlled system for an active ankle-foot prosthesis: an initial experimental study," in 9th International Conference on Rehabilitation Robotics, 2005. ICORR 2005. IEEE, 2005, pp. 375–379.

[11]. Huang S and Huang H., "Voluntary control of residual antagonistic muscles in transtibial amputees: Feedforward ballistic contractions and implications for direct neural control of powered lower limb prostheses," IEEE Transactions on Neural Systems and Rehabilitation Engineering, vol. 26, no. 4, pp. 894–903, 2018. [PubMed: 29641394]

[12]. Shu T, Huang SS, Shallal C, and Herr HM, "Restoration of bilateral motor coordination from preserved agonist-antagonist coupling in amputation musculature," Journal of NeuroEngineering and Rehabilitation, vol. 18, no. 1, pp. 1–17, 12 2021. [PubMed: 33397401]

[13]. Huang S and Ferris DP, "Muscle activation patterns during walking from transtibial amputees recorded within the residual limb-prosthetic interface," Journal of neuroengineering and rehabilitation, vol. 9, no. 1, p. 55, 2012. [PubMed: 22882763]

[14]. Hefferman GM, Zhang F, Nunnery MJ, and Huang H., "Integration of surface electromyographic sensors with the transfemoral amputee socket: A comparison of four differing configurations," Prosthetics and orthotics international, vol. 39, no. 2, pp. 166–173, 2015. [PubMed: 24469430]

[15]. Silver-Thorn B, Current T, and Kuhse B., "Preliminary investigation of residual limb plantarflexion and dorsiflexion muscle activity during treadmill walking for trans-tibial amputees," Prosthetics and orthotics international, vol. 36, no. 4, pp. 435–442, 2012. [PubMed: 22581661]

[16]. Rogers E, "Neurally-controlled ankle-foot prosthesis with non-backdrivable transmission for rock climbing augmentation," Master's thesis, Massachusetts Institute of Technology, 2019.

[17]. Rogers EA, Carney ME, Yeon SH, Clites TR, Solav D, and Herr HM, "An ankle-foot prosthesis for rock climbing augmentation." IEEE Transactions on Neural Systems and Rehabilitation Engineering, vol. 29, pp. 41–51, 2021. [PubMed: 33095704]

Author Manuscript Author Manuscript Author Manuscript Author Manuscript

[18]. Young A, Kuiken T, and Hargrove L., "Analysis of using emg and mechanical sensors to enhance intent recognition in powered lower limb prostheses," Journal of neural engineering, vol. 11, no. 5, p. 056021, 2014. [PubMed: 25242111]

[19]. Huang S., "Continuous proportional myoelectric control of an experimental powered lower limb prosthesis during walking using residual muscles." Ph.D. dissertation, 2014.

[20]. Hoover CD, Fulk GD, and Fite KB, "The design and initial experimental validation of an active myoelectric transfemoral prosthesis," Journal of Medical Devices, vol. 6, no. 1, 2012.

[21]. Yeon SH, Shu T, Rogers EA, Song H, Hsieh T-H, Freed LE, and Herr HM, "Flexible dry electrodes for emg acquisition within lower extremity prosthetic sockets," in 2020 8th IEEE RAS/EMBS International Conference for Biomedical Robotics and Biomechatronics (BioRob). IEEE, 2016, pp. 1088–1095.

[22]. Chi YM, Jung T, and Cauwenberghs G., "Dry-contact and noncontact biopotential electrodes: Methodological review," IEEE reviews in biomedical engineering, vol. 3, pp. 106–119, 2010. [PubMed: 22275204]

[23]. Lin C-T, Liao L-D, Liu Y-H, Wang I-J, Lin B-S, and Chang J-Y, "Novel dry polymer foam electrodes for long-term eeg measurement," IEEE Transactions on Biomedical Engineering, vol. 58, no. 5, pp. 1200–1207, 2010. [PubMed: 21193371]

[24]. Wang L-F, Liu J-Q, Yang B, and Yang C-S, "Pdms-based low cost flexible dry electrode for long-term eeg measurement," IEEE Sensors Journal, vol. 12, no. 9, pp. 2898–2904, 2012.

[25]. Jung H-C, Moon J-H, Baek D-H, Lee J-H, Choi Y-Y, Hong J-S, and Lee S-H, "Cnt/pdms composite flexible dry electrodesfor long-term ecg monitoring," IEEE Transactions on Biomedical Engineering, vol. 59, no. 5, pp. 1472–1479, 2012. [PubMed: 22410324]

[26]. Hoffmann K-P and Ruff R, "Flexible dry surface-electrodes for ecg long-term monitoring," in 2007 29th Annual International Conference of the IEEE Engineering in Medicine and Biology Society (EMBC). IEEE, 2007, pp. 5739–5742.

[27]. Peng H-L, Liu J-Q, Dong Y-Z, Yang B, Chen X, and Yang C-S, "Parylene-based flexible dry electrode for bioptential recording," Sensors and Actuators B: Chemical, vol. 231, pp. 1–11, 2016.

[28]. Chlaihawi AA, Narakathu BB, Emamian S, Bazuin BJ, and Atashbar MZ, "Development of printed and flexible dry ecg electrodes," Sensing and bio-sensing research, vol. 20, pp. 9–15, 2018.

[29]. Zhang H, Pei W, Chen Y, Guo X, Wu X, Yang X, and Chen H., "A motion interference-insensitive flexible dry electrode," IEEE Transactions on Biomedical Engineering, vol. 63, no. 6, pp. 1136–1144, 2015. [PubMed: 26441439]

[30]. Chan AD and Lemaire ED, "Flexible dry electrode for recording surface electromyogram," in 2010 IEEE Instrumentation & Measurement Technology Conference Proceedings. IEEE, 2010, pp. 1234–1237.

[31]. Stegeman D and Hermens H, "Standards for surface electromyography: The European project Surface EMG for Non-invasive Assessment of Muscles (SENIAM)," Enschede: Roessingh Research and Development, pp. 108–12, 2007.

[32]. Young AJ, Hargrove LJ, and Kuiken TA, "The effects of electrode size and orientation on the sensitivity of myoelectric pattern recognition systems to electrode shift," IEEE Transactions on Biomedical Engineering, vol. 58, no. 9, pp. 2537–2544, 2011. [PubMed: 21659017]

[33]. De Luca CJ, Kuznetsov M, Gilmore LD, and Roy SH, "Inter-electrode spacing of surface emg sensors: reduction of crosstalk contamination during voluntary contractions," Journal of biomechanics, vol. 45, no. 3, pp. 555–561, 2012. [PubMed: 22169134]

[34]. DuPont de Nemours, Inc., ""KAPTON" POLYIMIDE FILM, H TYPES, V TYPES. AND VARIAIONS, MSDS No. DU005413," 5 2011, "https://cpb-us-e1.wpmucdn.com/sites.usc.edu/dist/a/194/files/2018/07/Polyimide-2dw4nvf.pdf", Accessed 15 Feb 2020.

[35]. McAvoy M, Tsosie JK, Vyas KN, Khan OF, Sadtler K, Langer R, and Anderson DG, "Flexible multielectrode array for skeletal muscle conditioning, acetylcholine receptor stabilization and epimysial recording after critical peripheral nerve injury," Theranostics, vol. 9, no. 23, pp. 7099–7107, 2019. [PubMed: 31660089]

Author Manuscript Author Manuscript Author Manuscript Author Manuscript

[36]. Constantin CP, Aflori M, Damian RF, and Rusu RD, “Biocompatibility of polyimides: A mini-review,” Materials, vol. 12, no. 19, p. 3166, 2019.

[37]. Posada-Quintero H, Rood R, Burnham K, Pennace J, and Chon K., “Assessment of carbon/salt/adhesive electrodes for surface electromyography measurements,” IEEE J Transl Eng Health Med, vol. 4, no. 2100209, 2016.

[38]. Jiang Y, Samuel O, Liu X, Wang X, Idowu P, Li P, Chen F, Zhu M, Geng Y, Wu F et al. , “Effective biopotential signal acquisition: comparison of different shielded drive technologies,” Applied Sciences, vol. 8, no. 2, p. 276, 2018.

[39]. Yeon SH, “Design of an advanced sEMG processor for wearable robotics applications,” Master’s thesis, Massachusetts Institute of Technology, 2019.

[40]. Arvidsson A, Grassino A, and Lindstrom L., “Automatic selection of uncontaminated electromyogram as applied to respiratory muscle fatigue,” Journal of Applied Physiology, vol. 56, no. 3, pp. 568–575, 1984. [PubMed: 6706766]

[41]. Yeon SH and Herr HM, “Rejecting impulse artifacts from surface emg signals using real-time cumulative histogram filtering,” in 2021 43rd Annual International Conference of the IEEE Engineering in Medicine and Biology Society (EMBC). IEEE, 2021, to appear.

[42]. Wolf EJ, Cruz TH, Emondi AA, Langhals NB, Naufel S, Peng GC, Schulz BW, and Wolfson M., “Advanced technologies for intuitive control and sensation of prosthetics,” Biomedical engineering letters, vol. 10, no. 1, pp. 119–128, 2020. [PubMed: 32175133]

[43]. Yamagami M, Peters KM, Milovanovic I, Kuang I, Yang Z, Lu N, and Steele KM, “Assessment of dry epidermal electrodes for long-term electromyography measurements,” Sensors, vol. 18, no. 4, p. 1269, 2018.

[44]. Brinton MR, Barcikowski E, Davis T, Paskett M, George JA, and Clark GA, “Portable take-home system enables proportional control and high-resolution data logging with a multi-degree-of-freedom bionic arm,” Frontiers in Robotics and AI, vol. 7, 2020.

[45]. Lee S, Jamil B, Kim S, and Choi Y., “Fabric vest socket with embroidered electrodes for control of myoelectric prosthesis,” Sensors, vol. 20, no. 4, p. 1196, 2020.

Author Manuscript Author Manuscript Author Manuscript Author Manuscript

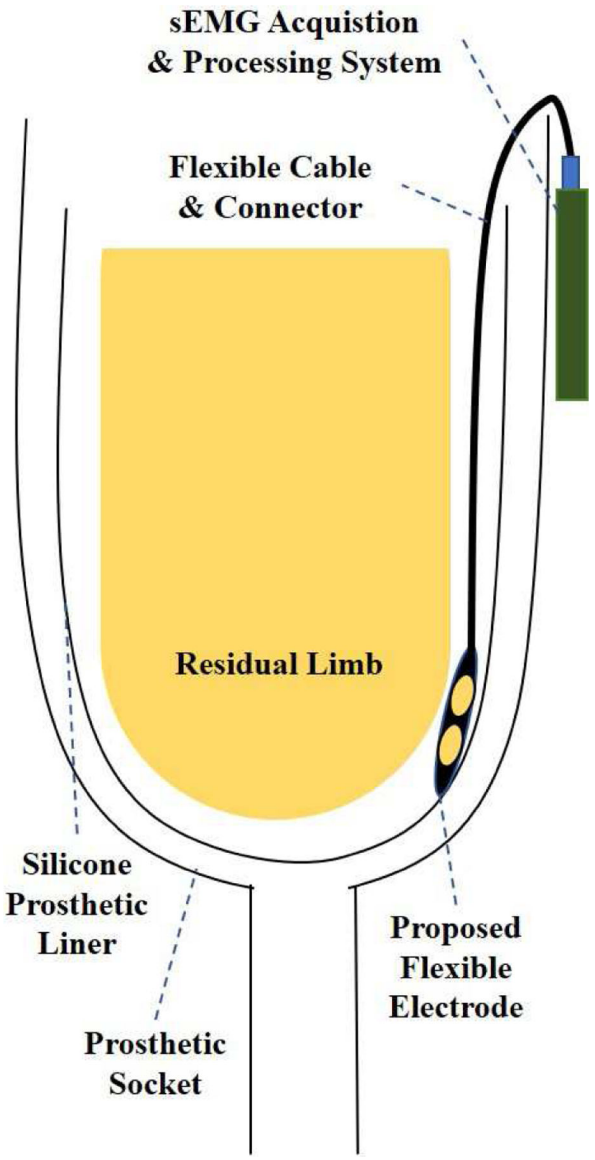

Fig. 1.

SLIP electrode design concept showing electrode worn against the skin of the residuum inside a standard silicone prosthetic liner. An integrated, flexible cable and connector allows the sensor to interface with an acquisition and processing system mounted externally on the socket.

Author Manuscript Author Manuscript Author Manuscript Author Manuscript

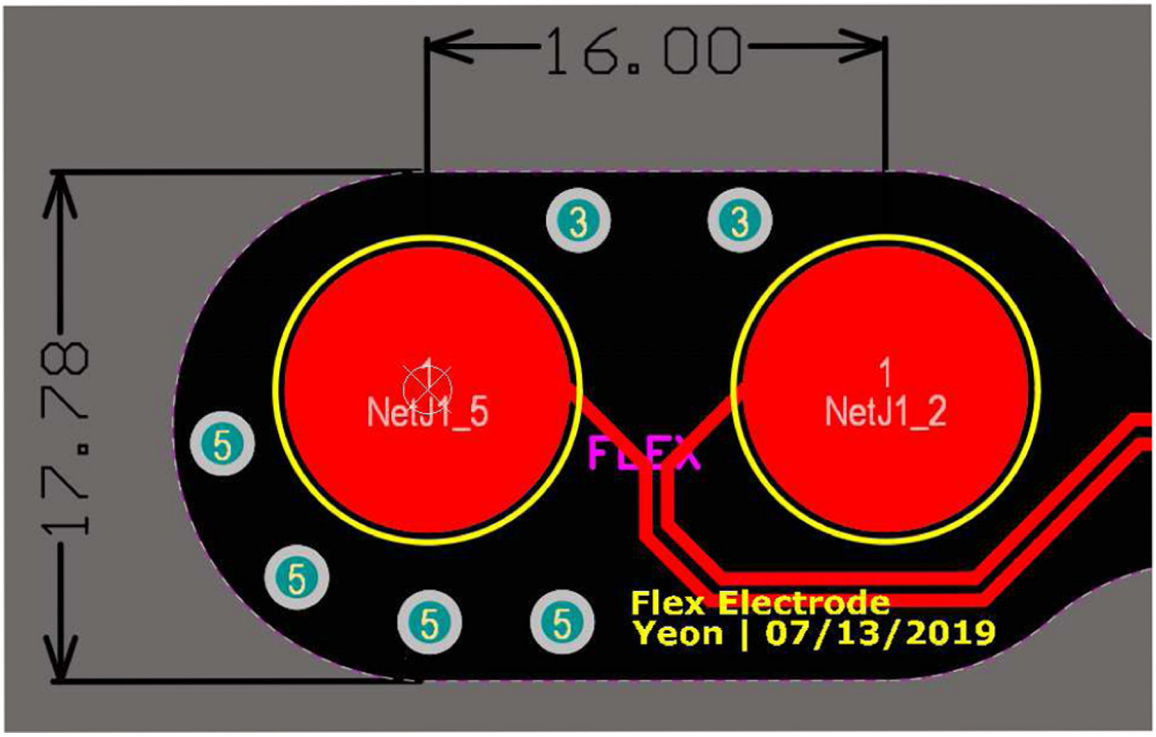

Fig. 2.

Electrical model of the novel electrode. Each bipolar electrode has a diameter of 10 mm and inter-electrode distance of 16mm. Mechanical holes on the electrode were placed for potential anchoring and mounting inside a prosthetic liner or sock.

Author Manuscript Author Manuscript Author Manuscript Author Manuscript

Fig. 3.
Fabricated prototype of the novel electrode. (a) Size comparison of the electrode. (b,c) Demonstration of manufactured electrode flexibility.

Author Manuscript Author Manuscript Author Manuscript Author Manuscript

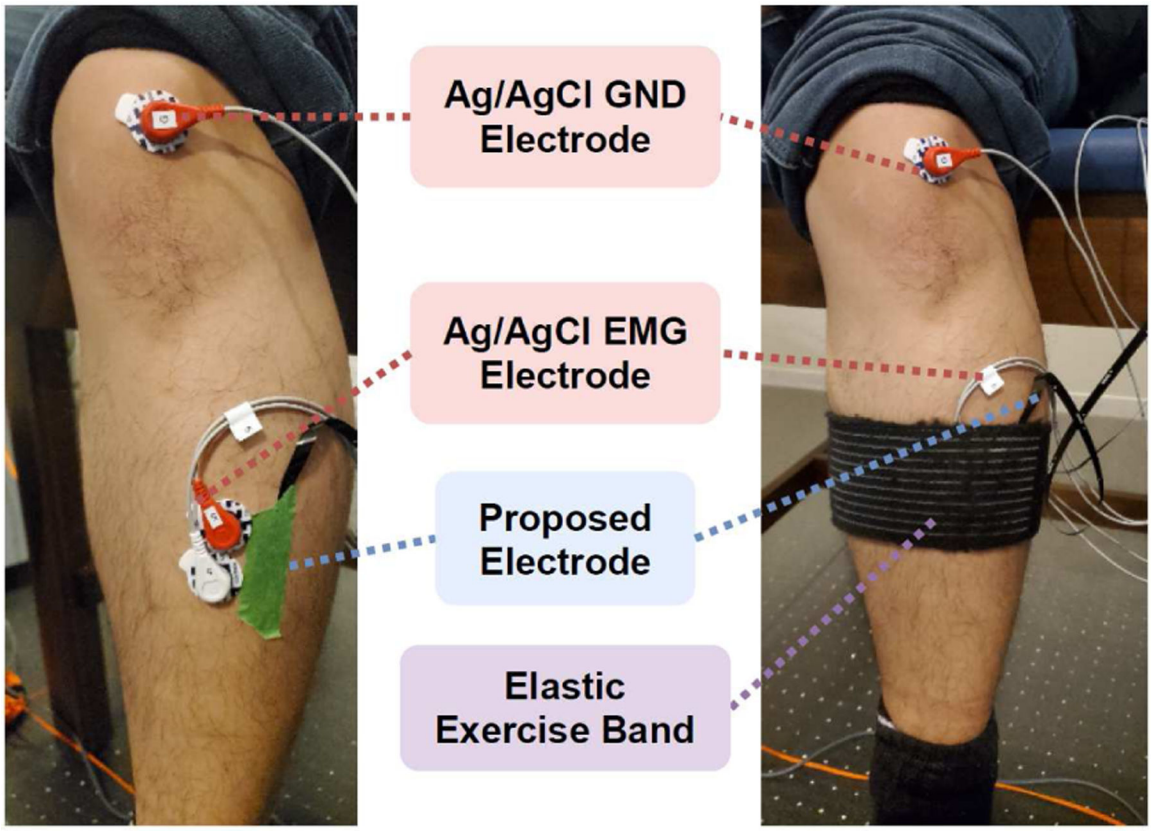

Fig. 4.

Example electrode configuration across the TA with Ag/AgCl electrodes in the medial position. An adhesive piece of tape is applied on top of the flexible electrode to ensure proper placement. Elastic exercise band applying uniform pressure to all electrodes.

Author Manuscript Author Manuscript Author Manuscript Author Manuscript

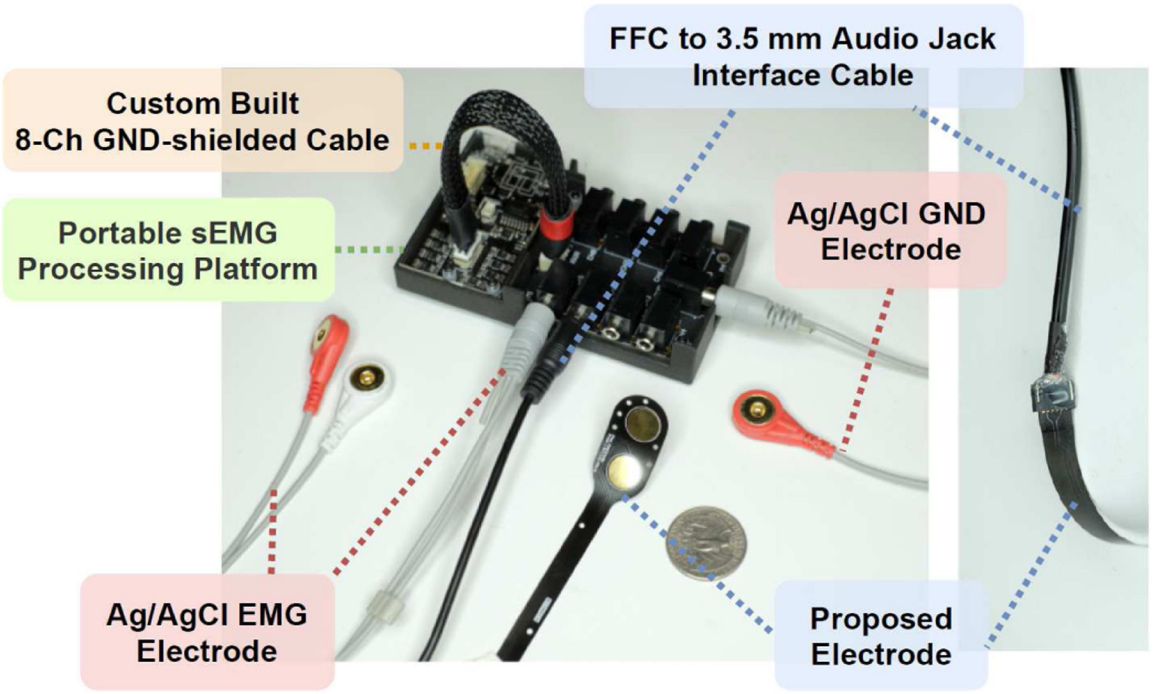

Fig. 5.

Embedded 8-channel sEMG acquisition and processing platform used for evaluation with example Ag/AgCl bipolar pair, SLIP electrode, and ground electrode attached.

Author Manuscript Author Manuscript Author Manuscript Author Manuscript

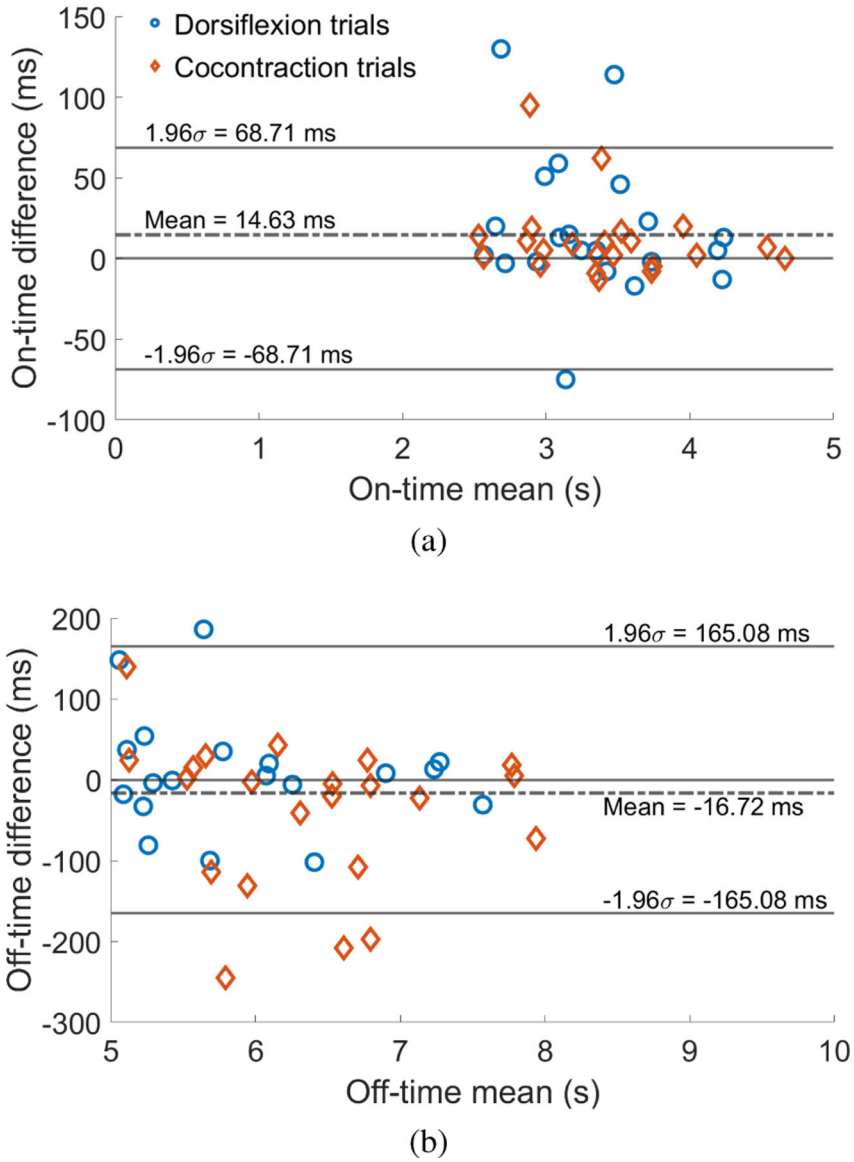

Fig. 6.

Bland-Altman plots of (a) relative muscle activity on-time and (b) relative muscle activity off-time. Positive differences indicate earlier detection by the SLIP electrode compared to commercial Ag/AgCl electrodes. Blue circles indicate differences from dorsiflexion trials (n= 22) while orange diamonds indicate differences from cocontraction trials (n= 21).

Author Manuscript Author Manuscript Author Manuscript Author Manuscript

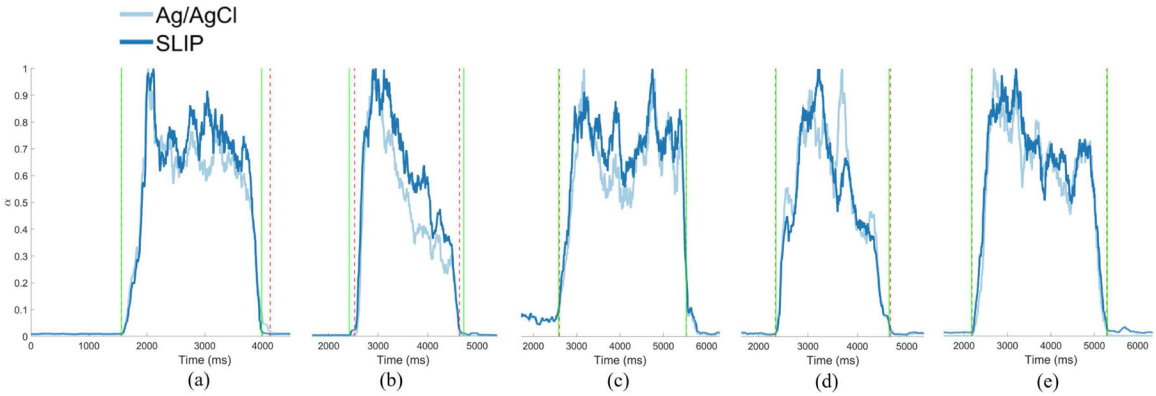

Fig. 7.

(a-e) Representative TA muscle activations (a) processed from data collected during dorsiflexion trials for each of subjects 1–5. Vertical dashed red lines indicate on- and off-times calculated with data from the Ag/AgCl electrodes. Vertical solid green lines indicate on- and off-times calculated with data from the SLIP electrode.

Author Manuscript Author Manuscript Author Manuscript Author Manuscript

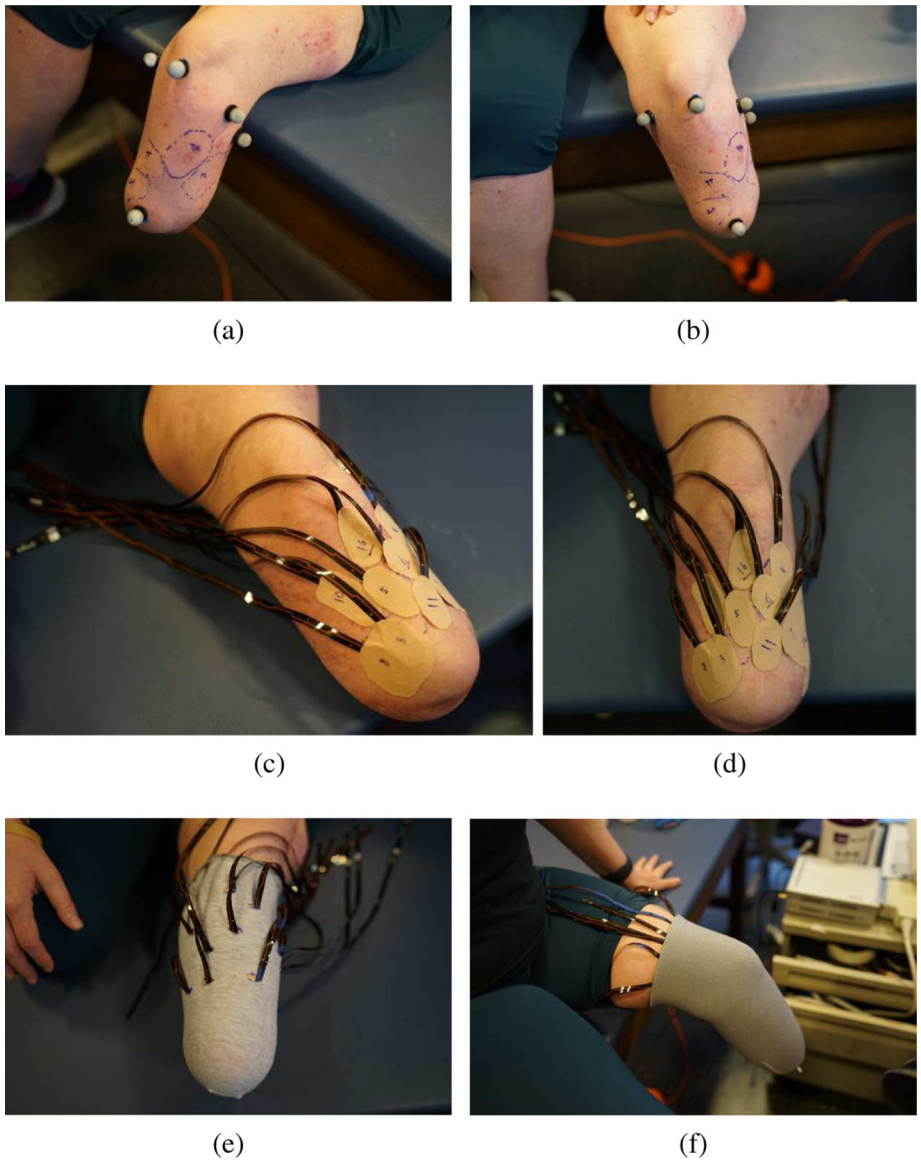

Fig. 8.

Example use case of the SLIP electrodes within an LE prosthetic liner. The 16 SLIP electrodes are placed and attached on the residual limb. This figure does not represent the actual instrumentation setup of the Experiment B. (a,b) Preparation of the residual limb's skin surface. Corresponding target musculature are labeled and bony anatomical landmarks are marked upon the skin's surface. (c,d) Electrodes are placed on the surface of the residual limb using Kinesio tape. (e) Leads of the SLIP electrodes are routed through the prosthetic sock with modified holes. (f) Fully routed SLIP electrodes under the prosthetic liner.

Author Manuscript Author Manuscript Author Manuscript Author Manuscript

Fig. 9.

Example use case of the embedded 16-channel sEMG acquisition and processing platform. The sEMG system is connected to the 16 electrodes as configured in Fig. 8f. This setup does not represent the actual instrumentation setup of the Experiment B, which only instrumented the four muscles of the AMI muscle pairs.

Author Manuscript Author Manuscript Author Manuscript Author Manuscript

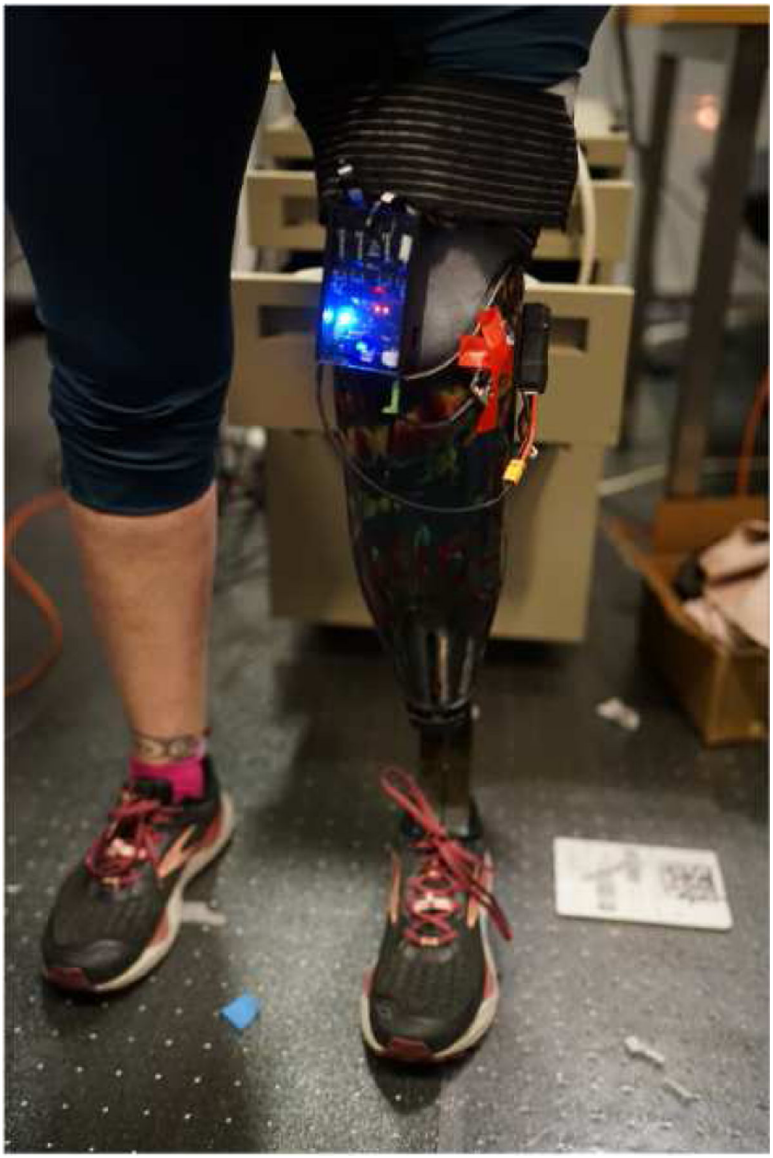

Fig. 10.

Portable sEMG measurement setup used for Experiment B during both stationary voluntary movement and ambulation. Four SLIP electrodes interface with the four muscles of the AMI muscle pairs (TA-LG and PL-TP).

Author Manuscript Author Manuscript Author Manuscript Author Manuscript

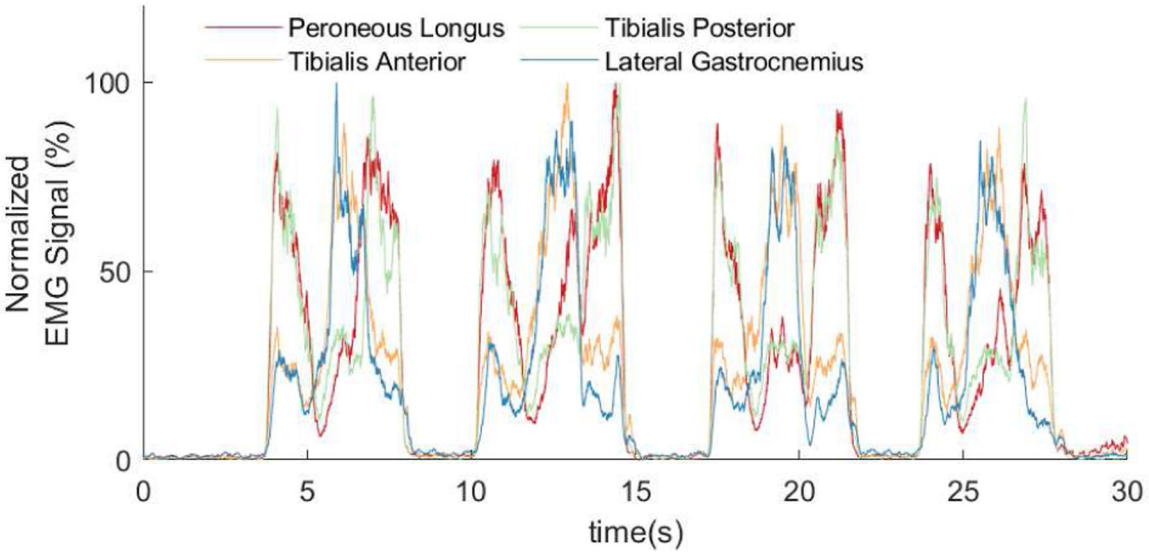

Fig. 11.

Measured and normalized sEMG signals from the four SLIP electrodes over target AMI muscle pairs (TA-LG and PL-TP) during voluntary clockwise rotations of the phantom ankle and subtalar joints.

Author Manuscript Author Manuscript Author Manuscript Author Manuscript

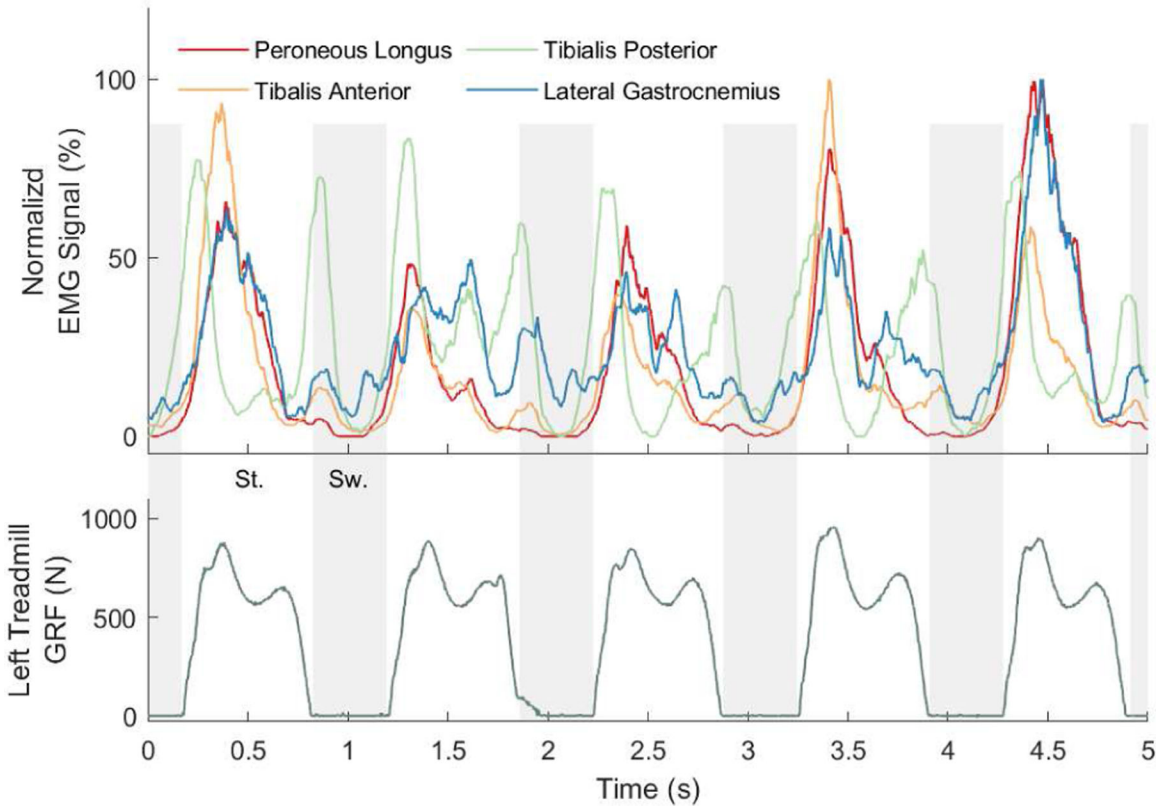

Fig. 12.

Signals measured using the 16-channel sEMG processing platform with four electrodes over target AMI muscle pairs during treadmill walking at a speed of 1.4 m/s. The measured raw sEMG signal, processed sEMG signal, and ground reaction force (GRF) data are shown. Cyclic and repetitive muscle activation patterns correlating with GRF are demonstrated. Stance phases are presented with a white background while swing phases are presented with a gray background.

Author Manuscript Author Manuscript Author Manuscript Author Manuscript

(a)

(b)

Fig. 13.

Skin of the residual limb after one hour of weight-bearing ambulation. Skin indentation and irritation are not visible where electrodes were placed.

Author Manuscript Author Manuscript Author Manuscript Author Manuscript

Fig. 14.

Electrode configurations for user comfort evaluation: (a) SLIP electrodes; (b) Commercial Ag/AgCl electrodes without connectors and wires; (c) Commercial Ag/AgCl electrodes with connectors and wires

Author Manuscript

Author Manuscript

Author Manuscript

Author Manuscript

TABLE I

ELECTRODE DESIGN SPECIFICATIONS

Specification	Value
Electrode Type	Bipolar
Electrode Surface Diameter	10.00 mm
Inter-Electrode Distance	16.00 mm
Electrode Surface	Gold Plating
Width	17.78 mm
Length	598.81 mm
Connector	6-pin FFC

Author Manuscript

Author Manuscript

Author Manuscript

Author Manuscript

TABLE II

ELECTRODE MATERIAL SPECIFICATIONS

Base Substrate	Polyimide Film
Conductor	Copper Film (0.3 ~ 0.5 oz)[1]
Electrode Surface Finish	Gold Plating
Thickness	80~100 μm[1]

[1] Varies between manufacturers

Author Manuscript

Author Manuscript

Author Manuscript

Author Manuscript

TABLE III

REPORTED COMFORT AND PREFERENCE SCORES

Perception	Activity	SLIP Electrode	Ag/AgCl Only	Ag/AgCl + Cable
Comfort [1]	Sitting	5	3	1
	Standing	5	4	1
	Walking (1.4 m/s)	5	3	1
	Stair Ascent	5	4	1
	Stair Descent	5	4	1
	Overall	5	3	1
Level of socket suspension [1]		5	5	1
Preference for daily life usage [1]		5	3	1

[1] 1-not applicable; 5-same as prescribed prosthesis without electrodes.